



Available online at www.sciencedirect.com



CONTINENTAL SHELF
RESEARCH

Continental Shelf Research 24 (2004) 627–642

www.elsevier.com/locate/csr

Shallow gas in shelf sediments of the Namibian coastal upwelling ecosystem

K.-C. Emeis^{a,*}, V. Brüchert^b, B. Currie^c, R. Endler^a, T. Ferdelman^b, A. Kiessling^a, T. Leipe^a, K. Noli-Peard^c, U. Struck^d, T. Vogt^a

^a Institut für Ostseeforschung Warnemünde, Seestr. 15, Warnemünde 18119, FRG

^b Max-Planck-Institut für Marine Mikrobiologie Bremen, Celsiusstr. 1, Bremen 28359, FRG

^c Ministry of Fisheries and Marine Resources of Namibia (MFMR), National Marine Information and Research Centre (NatMIRC), Swakopmund, Namibia

^d Ludwig-Maximilian-Universität München, Richard-Wagner-Str. 10, München 80333, FRG

Received 19 February 2003; received in revised form 5 November 2003; accepted 30 January 2004

Abstract

Outbreaks of toxic H₂S gas are a seasonally recurrent feature in the near-shore environment of Namibian shelf. They potentially have a significant economic and societal relevance because of their effects on biota in one of the largest marine coastal upwelling regions. Until recently they were considered to be of local geographical extent and forced by processes in the water column. Here, we report on ship-borne acoustic surveys and core evidence that suggest a significant contribution by eruptions of biogenic gas accumulations in unconsolidated organic-rich diatomaceous oozes on the shelf. Approximately 8% of the mud area (1360 km²) hosts free gas just decimeters to meters below the sediment–water interface. The gas is a mixture of methane and H₂S. A portion of the H₂S is produced by the reduction of sulfate with methane in the sulfate–methane transition zone, where it reaches pore water concentrations up to 18 mmol/l. The gas is contained in very porous, low density and liquid sediments and is in some cases capped by a denser layer within the sediment.

Possible candidates to trigger eruptions are changes in the atmospheric and oceanographic pressure fields, shoaling of the methane–sulfate transition zone caused by decreasing rates of methane oxidation, and precipitation-induced pressure signals from the inland catchment transmitted to the base of the diatomaceous ooze via fossil river beds.

© 2004 Elsevier Ltd. All rights reserved.

Keywords: Hydrogen sulfide; Methane; Shallow gas; Sediments; Namibia; Benguela region; SE Atlantic Ocean

1. Introduction

The Benguela coastal upwelling system is one of the classical eastern boundary current systems that

are among the most biologically productive regions of the World ocean. It has recently been established as a Large Marine Ecosystem and is jointly managed by the states of Angola, Namibia, and South Africa. A remarkable feature of the Namibian coast is events of hydrogen sulfide pervading the coastal waters and near-shore land (Copenhagen, 1953; Weeks et al., 2002). Although not a regular feature, most outbreaks appear to coincide with specific climatic and associated

*Corresponding author. Institut für Biogeochemie und Meerschemie, Universität Hamburg, Bundesstrasse 55, Hamburg 20146, Germany. Tel.: +49-40-42838-4992; fax: +49-40-42838-6347.

E-mail address: emeis@geowiss.uni-hamburg.de
(K.-C. Emeis).

weather patterns in austral summer and have a—possibly spurious—correlation with inland rains (Reuning, 1925). The sulfide outbreaks are suspected to be a major and sometimes catastrophic influence on coastal and pelagic habitats in the shelf ecosystem (Copenhagen, 1953; Weeks et al., 2002). Geographical regions on the shelf with the highest incidence of observed eruptions also coincide with nursery grounds of important pelagic and demersal fish; in 1992/93 half of the recruit population of cape hake (two billion individuals) was eradicated by anoxic conditions, possibly in connection to sulfide eruptions. Until recently, sulfide outbreaks have been attributed to processes in the water column (Bailey, 1991; Copenhagen, 1953).

Here we show that an alternative source of H_2S may be gas-laden sedimentary deposits on the shelf. Sediments rich in opal and organic carbon are deposited in a narrow belt on the inner shelf beneath the upwelling area off Namibia. Their distribution and facies are determined by water depth, the current and wave energy at the sea floor, biological productivity (both pelagic and benthic), terrigenous input, and diagenesis (Bremner, 1983). Biogeochemical processes at the sediment–water interface are determined by very high accumulation rates of organic material which result in high oxygen consumption rates and high sulfate reduction rates at the sea floor (Brüchert et al., in press; Ferdelman et al., 1999). Based on results of an acoustic survey and coring in August of 2000, we propose that eruptions of methane and H_2S originating from unconsolidated, gas-charged sediments are an important source of H_2S . This view is supported by reports of ephemeral mud islands that have been sighted in the near-coastal zone in the years 1900, 1959, and 2000.

2. Methods

All data were acquired during expedition R/V *METEOR* 48-2 (5–23 August, 2000). Fig. 1 depicts track lines, the extent of the diatomaceous mud according to PARASOUND, and stations for water column and sediment work.

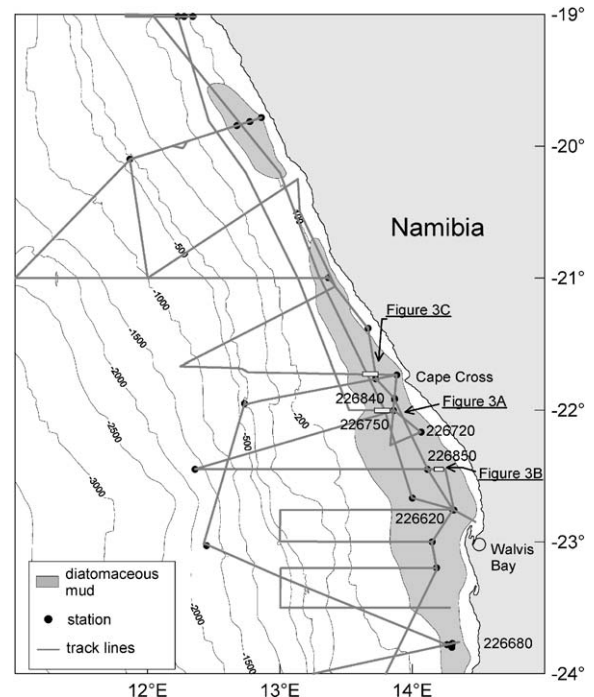


Fig. 1. Station map of F/S Meteor expedition 48-2 (August 2000) with track lines of PARASOUND surveys, and the extent of diatomaceous mud on the shelf (modified from Bremner, 1983 and new data). Station numbers refer to locations discussed in the text. Rectangles mark the PARASOUND profile segments shown in Fig. 3.

2.1. Acoustic surveys

Seafloor morphology, sediment distribution, and layering of sediments were investigated using the PARASOUND subbottom profiling system on R/V *METEOR*. Detailed technical descriptions of the acoustic systems are given in Spieß (1993). PARASOUND seismograms were digitized, pre-processed, printed and stored on hard disk in a modified SEG-Y-format using the Paradigma System. A frequency of 4 kHz and a pulse length of two periods were used during the whole cruise. Additional measurements with different frequencies (2.5–5.5 kHz) and pulse lengths of 1–6 periods were performed at coring stations in order to study the influence of frequency and pulse length of the source signal on the reflection pattern. The acoustic data were acquired in straight lines to get cross-sections of the sub-bottom structure.

2.2. Water column work

CTD-profiles and water samples were obtained during the cruise with help of a complete SBE 911+(Sea-Bird Electronics Inc., USA) CTD system equipped with sensors for pressure, conductivity, temperature, oxygen, and a HAARDT-fluorometer for measuring chlorophyll and turbidity. The sensors were connected to a rosette water sampler containing 12 5-l bottles (HYDROBIOS, Kiel, Germany).

Samples taken from bottom water were analyzed for dissolved oxygen and hydrogen sulfide. Sample depths were selected at the oxygen minima and/or turbidity maxima based on CTD profiles. Also analyzed were samples from the supernatant water of multicores (see below). Samples were immediately fixed for oxygen content analysis according to the Winkler method, and for hydrogen sulfide using 20% zinc acetate. Winkler titrations for oxygen used a visual endpoint detection (detection limit 0.07 ml/l), sulfide was determined by a spectrophotometric method (Cline, 1969); both were carried out on board.

2.3. Coring devices

Sediment samples were retrieved by multicorer and van-Veen grab sampler at 31 stations in the shelf area and on the upper continental slope off Namibia between 25°30'S and 19°47'S. At selected stations, we also obtained long sediment cores with a gravity corer (Table 1). For the sampling of complete and undisturbed sediment surfaces and the overlying bottom water, we used a multicorer equipped with 8 large tubes (10-cm outer, 9.6-cm inner diameter) and 4 small tubes (8 cm, 7.6-cm inner diameter) of 80-cm length.

2.4. Pore water analyses

Stations 226620, 226680, 226750, and 226840 (close to 226750) were selected for detailed pore-water and gas profiling. Stations 226680 and 226750 were selected based on PARASOUND depth profiles that indicated a shallow reflector at 4–5-m sediment depth with a gas-rich zone below. By contrast, gas-rich zones were not indicated

by the PARASOUND at stations 226620 and 226840.

The gravity cores were cut into 100 cm sections on deck after core retrieval. Immediately after the sediment was cut, a 3 cm³ sediment plug was taken from the cut ends of the sections and added to 5 ml of 2.5% NaOH in a serum vial. The vial was capped with a butyl rubber stopper and sealed with an aluminum crimp for immediate measurement of the CH₄ concentration in the headspace. This procedure allowed, within minutes after the core came on deck, an approximate determination in which section the sulfate–methane transition zone was located. For detailed profiling, the cores were extruded with a whole core piston and sampled every 10 cm to the sulfate-transition zone, then in 5-cm intervals across the transition into the methanogenic zone which was identified by its porous texture. Below this depth, samples were taken every 15 cm to the bottom of the core.

Pore water was squeezed pneumatically under air at in situ temperatures through 0.4 µm nitrate-free Millipore cellulose acetate filters into 10-ml glass syringes taking care to avoid the development of air bubbles. A 1-ml sub-sample was fixed with 300-µl 20% zinc acetate for the determination of dissolved sulfate and sulfide.

Methane and dissolved sulfide were analyzed in the ship laboratory. A 500- or 1000-µl sub-sample was withdrawn from the headspace of the serum vial with a syringe and analyzed by an HP 5890 gas chromatograph equipped with a flame ionization detector. Dissolved sulfide concentration was determined spectrophotometrically at a wavelength of 670 nm using the methylene blue method (Cline, 1969). After adequate dilution to achieve absorptions in the linear range of this method, the zinc acetate-fixed pore-water was derivatized with phenylethylene diamine and kept for 3 h in the dark before analysis. Concentrations were determined after daily calibration with ZnS suspensions having concentrations of 2.65 and 26.5 µmol/l.

In order to account for the possible loss of surface sediment during gravity coring, cores from Stations 226620, 226680, and 226750 were squeezed in a glove bag, and also analyzed for

Table 1

Core locations, water depths, identification of cores with pore water data and whether gas was detected by PARASOUND at the coring location

Station number	Latitude	Longitude	Water depth (m)	MUC recovery (cm)	SL recovery (cm)	Pore waters	Gas in PARASOUND
226620	22°45.51'S	014°18.87'E	83	51	400	X	No
226630	23°00.00'S	014°08.98'E	121	60	264		Yes
226640	23°11.80'S	014°11.02'E	118	54	431		Yes
226650	25°28.02'S	013°05.05'E	1781	27	n.t.		No
226660	24°06.45'S	012°45.94'E	1821	25	563		No
226670	23°46.30'S	014°18.17'E	107	54	436		Yes
226680	23°46.52'S	014°17.96'E	109	53	455	X	Yes
226690	23°46.81'S	014°15.74'E	109	49	380		No
226700	23°01.70'S	012°26.76'E	1800	16	n.t.		No
226710	21°56.93'S	012°43.95'E	379	30	n.t.		No
226720	22°09.98'S	014°04.07'E	69	51	348		No
226730	22°00.17'S	013°51.52'E	91	50	420		Yes
226740	21°55.10'S	013°51.93'E	79	52	575		Yes
226750	21°54.70'S	013°51.96'E	77	48	350	X	Yes
226760	21°45.77'S	013°43.40'E	94	39	470		Yes
226770	21°22.97'S	013°40.00'E	51	49	526		Yes
226780	20°59.95'S	013°21.99'E	81	30	830		Yes
226790	19°47.00'S	012°51.61'E	50	51	480		No
226800	19°48.83'S	012°46.36'E	93	54	425		No
226810	19°50.66'S	012°40.50'E	116	46	340		No
226820	10°05.96'S	011°51.97'E	424	27	680		No
226830	21°44.00'S	013°53.02'E	35	36	680		Yes
226840	21°55.06'S	013°51.99'E	77	n.t.	n.t.	X	Yes
226850	22°27.01'S	014°06.97'E	95	57	360		Yes
226860	22°45.00'S	014°18.04'E	83	2	n.t.		No
226870	22°40.03'S	014°00.03'E	125	50	370		No
226880	19°00.97'S	012°20.62'E	98	31	n.t.		No
226890	19°01.00'S	012°16.54'E	109	40	n.t.		No
226900	19°01.01'S	012°13.74'E	119	33	n.t.		No
226910	22°00.19'S	013°51.51'E	90	5	340		No
226920	22°26.95'S	012°21.48'E	1683	20	1032		No

n.t. = not taken; MUC = multicorer; SL = gravity corer.

methane and dissolved sulfide. Then the sulfide and methane concentrations were used to estimate the amount of core loss during gravity coring.

2.5. Sediment physical properties

Upon arrival in the shore-based laboratory, the 1-m sections of cores were processed with a GEOTEK multi-sensor core logger that produces high-resolution datasets of sediment wet-bulk density (measured as gamma-ray attenuation relative to a standard). After logging the sections, they were cut lengthwise, and samples were taken to calibrate the density profiles from GRAPE

(gamma ray attenuation porosity evaluator) against densities of discrete samples. Water content and dry bulk densities of syringe samples with a known volume of 10 cm³ were determined by weighing before and after drying at 40°C. No salt correction was used.

3. Results

3.1. Dissolved oxygen and H₂s in the water column

Oxygen concentration in bottom waters at the inshore stations between 21°S and 23°S were

below detection. Oxygen levels below 0.5 ml/l (22.3 $\mu\text{mol/l}$) extended along the coast at depths shallower than 200 m from 23°25'S to the northernmost sampled station (19°S). Bottom oxygen levels increased offshore to a maximum value of 5.5 ml/l (245 $\mu\text{mol/l}$) at 1800 m. Hydrogen sulfide was present in high concentrations of up to 188 $\mu\text{mol/l}$ in the bottom water closely inshore between Walvis Bay (22°57'S) and Cape Cross (21°46'S) and to a water depth of 125 m (Fig. 2).

3.2. Results of PARASOUND echosoundings

The shelf off Namibia (water depth to about 150 m) is characterized by sedimentation of organic-rich diatomaceous ooze forming a NNW–SSE striking (coastal parallel) mud layer with a thickness of up to 14 m. The mud belt extends over 700 km in a N–S direction and 100 km in an E–W direction (Bremner, 1983). The spatial extent is shown in Fig. 1. Where no data were collected during the expedition, we

interpolated the extent of the mud belt from data given elsewhere (Bremner, 1983) and according to the surface sediment type encountered during a previous expedition with R/V Poseidon in 1999. The layer of the diatomaceous mud belt is almost acoustically transparent (Fig. 3A) and drapes the underlying relief to form an almost flat lens. Its base is a transgression conglomerate composed mainly of shell debris (see below) that is well imaged on the acoustic profiles by continuous high-amplitude reflection. The thickness of the diatomaceous mud is not uniform, exhibiting considerable small-scale variation in thickness in the area offshore Swakopmund and Walvis Bay. Here the mud belt is both widest, and the Holocene sediment layer is thickest. In total, the diatomaceous mud covers an area of approximately 18,000 km² with an estimated volume of 76 km³.

A conspicuous feature in many seismograms is acoustic blanking that is interpreted as gas accumulations at different depths and locations in the mud layer (Figs. 3B and C). This interpretation is supported by the identification of high concentrations of gas in cores from the affected areas (see below). Such features are common in gas-charged sediments and are caused by gas bubbles that scatter and attenuate the downward-travelling acoustic signals (Hovland and Judd, 1988). An acoustic shield is thus formed that masks the sedimentary structures below the reflector. The gas blanking is spotty in some profiles on the shelf offshore Namibia (Fig. 3B), whereas in other areas it is extensive and prevents any acoustic reflection of the mud over several kilometers (Fig. 3C). However, the gas accumulations are frequently patchy, because there are windows between individual gas occurrences through which the subsurface and the depth of the basal reflector can be traced (Fig. 3C).

Towards the west the area of mud accumulation area is bounded by a non-depositional/erosional area on the outer shelf. The sea floor here is characterized by either hard grounds or consolidated sediments. Well-stratified deposits with dipping reflectors are truncated and partly covered by silty/sandy sediments. Near the shelf break the

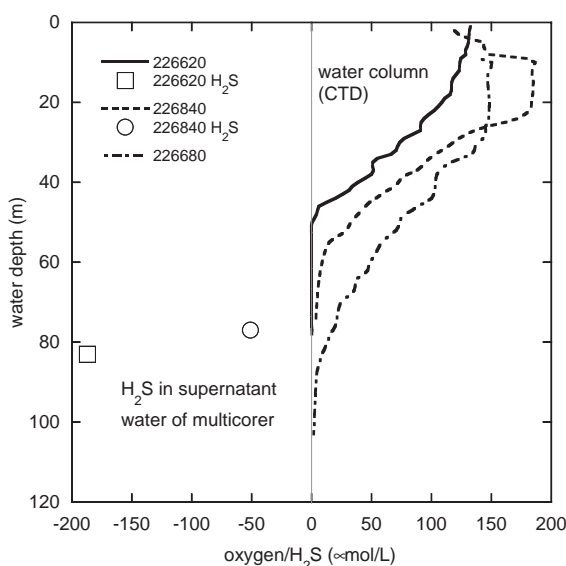


Fig. 2. CTD profiles of oxygen content in the water column of three stations. At all three stations, dissolved O₂ concentration reached 0 $\mu\text{mol/l}$ near the sea floor (lowest CTD readings 5 m above ground). At two stations (226620 and 226680), supernatant water of multicores (5–10 cm above sediment–water interface) contained H₂S (depicted as negative O₂).

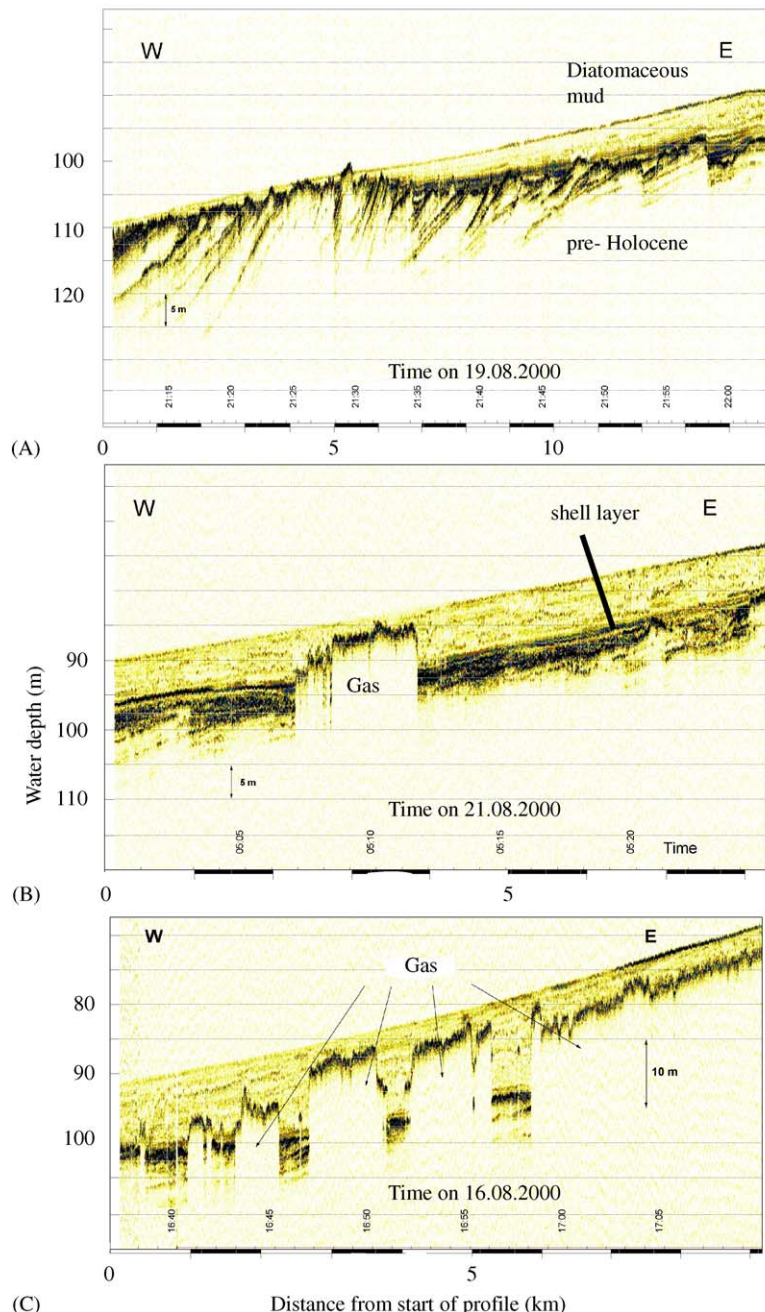


Fig. 3. Examples of PARASOUND echosounding depicting the vertical structure of sediments on the shelf offshore Namibia and features referred to in the text. For locations see Fig. 1.

environment changes again into a depositional regime. The transition is occasionally accompanied by ridge structures (possibly former beach

barriers). The upper slope facies is characterized by soft silts forming a smooth surface with westward prograding sediment layers.

We mapped the extent of gas-charged sediments based on the survey in August 2000 (Fig. 4) and found that their extent was significant (Table 2). They occupy a total area of 1350 km² and account for approximately 8% of the diatomaceous mud belt. Most significantly, the sector offshore Swakopmund and Walvis Bay that has the thickest mud accumulations also hosts abundant sedimentary gas accumulations. A comparison of sediment thickness with gas occurrence suggests that diatomaceous mud thickness is a key factor controlling the extent of the gas-charged zones. Whereas areas of diatomaceous mud less than 4 m thick contained virtually no free gas, sediments in areas where the mud was more than 12 m thick were completely gas-charged (Fig. 5).

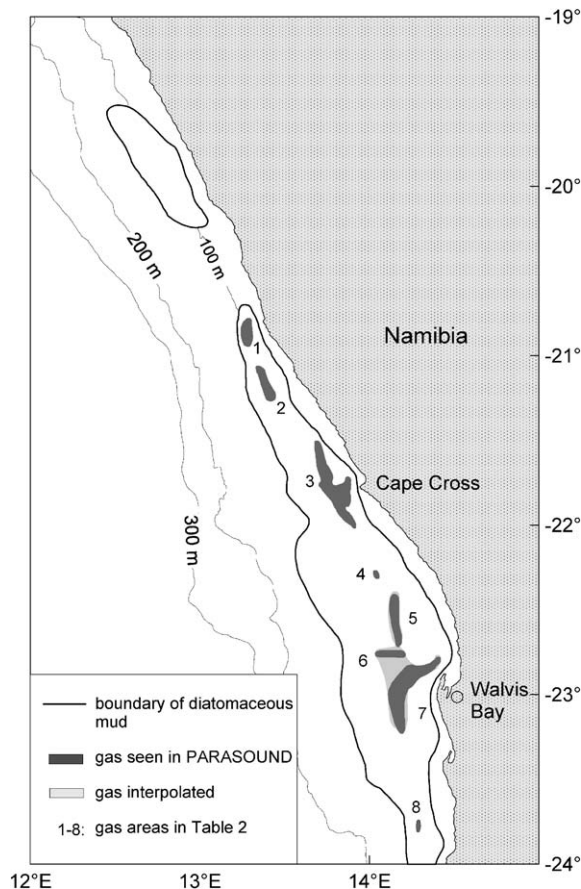


Fig. 4. Distribution of gas-charged diatomaceous mud based on PARASOUND echosounding. Numbers refer to areas given in Table 2.

3.3. Pore water composition

A 400 cm long gravity core and a 51 cm long multicore were retrieved from Station 226620 where PARASOUND gave no indication of gas in the sub-surface. Methane profiles of the gravity core from Station 226620 were determined to a depth of 350 cm and showed low concentrations of CH₄ throughout the core reaching a maximum concentration of 18 nmol CH₄/cm³ at a core depth

Table 2
Statistical evaluation of diatomaceous mud belt area occupied by gas charged sediments from PARASOUND

Area in Fig. 4	Area (km ²)	Percentage in area of diatomaceous mud
1	83.0	0.5
2	99.0	0.6
3	484.0	2.7
4	16.0	0.1
5	166.0	0.9
6	80.7	0.5
7	411.7	2.2
8	16.0	0.1
Sum	1357	7.6

Areas 1–8 are marked in Fig. 4.

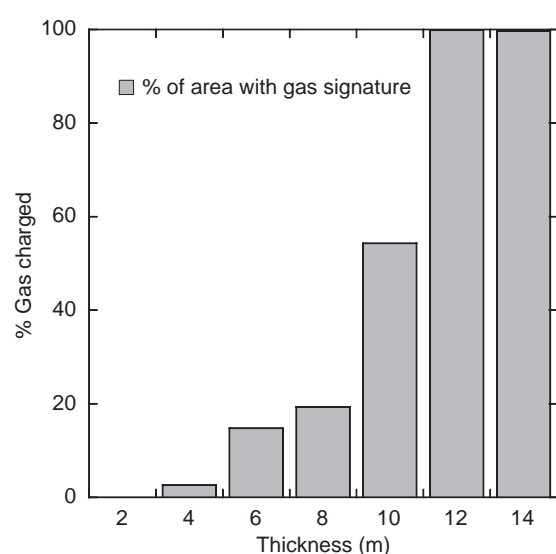


Fig. 5. Comparison of thickness of the diatomaceous mud from PARASOUND echosoundings with the occurrence of gas.

of 112 cm (Fig. 6A). There was no evidence of a sulfate-methane transition zone in this core, and sulfate was not consumed completely at the core bottom. The concentration of CH₄ decreased in the lowermost samples (Fig. 6B). It is unclear at present whether this decrease was due to the strong compaction and artificial loss of methane during gravity coring, or a real phenomenon. In contrast to methane, concentrations of sulfide were very high and reached concentrations of 7.2 mmol/l at 280 cm depth (Fig. 6A). The depth profile of dissolved sulfide suggested minimal loss of sediment during gravity coring. It is interesting to note that both the CH₄ and the hydrogen sulfide concentrations decreased in the lowermost three samples.

A 455 cm long gravity core was retrieved from Station 226680, which is located in an area where PARASOUND identified sub-surface gas accumulation. Comparison of sulfate and methane profiles from the multicorer and the gravity core suggested approximately 40 cm loss of surface sediment due to over-penetration in the gravity core. The sample depths in the gravity core were therefore corrected to account for this loss of sediment; these corrected depths are plotted in Figs. 6C and D. The highest sulfide concentrations (17.6 mmol/l) occurred at 120 cm in the core, 50 cm above the peak methane concentrations (Fig. 6C). The methane concentration data confirm the existence of free methane from depths of approximately 110 cm depth in the core, which was also indicated by gas escape structures in the very soft mud. Highest methane concentrations were found at 169 cm core depth (1650 nmol CH₄/cm³) (Fig. 6D).

A 350 cm long gravity core was retrieved from Station 226750. As for Station 226680, this station was selected because of a shallow acoustic reflector and a reflector-free zone below. In addition, the PARASOUND suggested the existence of rising gas bubbles through the water column. Comparison of sulfate and methane profiles from the multicorer and the gravity core also suggested loss of surface sediment of approximately 30 cm in the gravity core, and sample depths in the gravity core were again corrected to account for this loss of sediment accordingly. Sulfide concentrations

reached 16.3 mmol/l at 90 cm (Fig. 6E). The methane profile at this station showed an extremely sharp increase to a concentration above saturation from 86 to 90 cm sediment depth (Fig. 6F). Below this depth, concentrations remained constant at methane saturation, and the sediment texture, as in core 226680, was frothy and indicated the presence of free gas (maximum concentration 2900 nmol CH₄/cm³ at 269 cm depth).

Gravity core 226840 was taken in the immediate vicinity of station 226750, but at a site where PARASOUND did not indicate a shallow-subsurface reflector and where methane profiles were expected to be more gradual. Sulfide concentrations peaked at 135 cm (17.9 mmol/l) (Fig. 6G). Contrary to expectations, methane concentrations increased abruptly and reached super-saturation between 85 and 95 cm depth (Fig. 6H). No multicore was taken from this station, and therefore it remains uncertain whether sediment was lost during coring.

3.4. Sediment physical properties

The wet bulk densities and GRAPE densities show that the Holocene sediments in the diatomaceous mud belt are of low density (average of 5000 GRAPE determinations = 1.15 g cm⁻³, standard deviation ± 0.08 g cm⁻³) and are very rich in water (fractional porosities average 0.93, standard deviation ± 0.03). Examples of GRAPE-density logs for the upper 3 m of the Holocene diatomaceous ooze are shown in Fig. 7. Fig. 7A shows the density of gravity core 226680 where pore-water composition showed methane saturation. Fig. 7B depicts the density profile of gravity core 226850 taken in an area where acoustics showed gas accumulation. Fig. 7C shows the density profile for core 226720 where PARASOUND gave no indication of gas accumulation. From the profiles in Figs. 7A and B it appears that free gas accumulations are located where denser sediment overlies less dense and more porous sediments. We did not expect pronounced density fluctuations in cores where neither PARASOUND nor pore waters indicated free gas in the sediment. Indeed, variations in the density and porosity profiles of

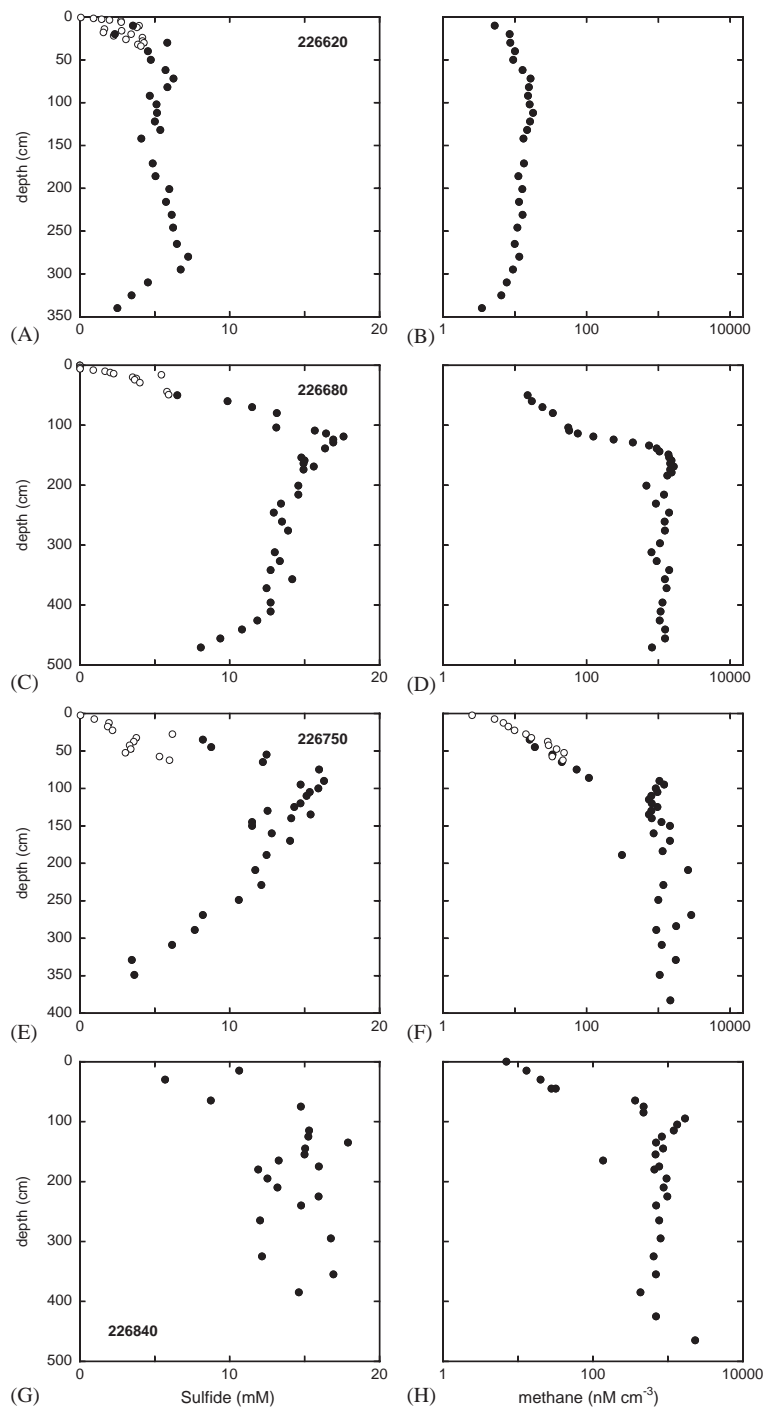


Fig. 6. Pore water profiles of sulfide and methane in 4 cores of the diatomaceous mud. Filled symbols denote samples from gravity cores, circles denote samples from multicores. Note log scale in B, D, F, and H. See Table 1 and Fig. 1 for locations.

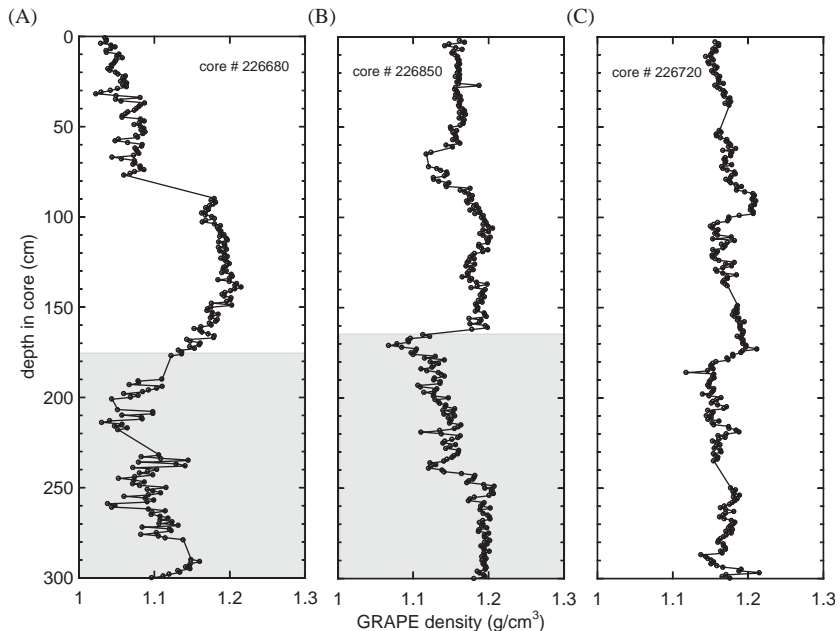


Fig. 7. Results of density measurements on whole cores (GRAPE) for core 226680 with methane supersaturation from pore water analyses in interval underlain in gray (A), for core 226850 from an area where PARASOUND indicated free gas in the sub-surface in the intervals underlain in gray (B), and for core 226720 where no gas was detected by PARASOUND.

core 226720 are comparatively smaller (between 1.1 and 1.2 g/cm^3) than in the two other cores. On the other hand, cores 226850 and 226720 displayed density variations of the same magnitude as cores from locations with gas (data not shown), but the coring locations had no gas signature in the acoustic survey.

To evaluate further the origin of denser sediment layers, we analyzed a set of sample across the dense sediment layer between 50 and 200 cm depth in core 226680 (Fig. 7A), because we speculated that the denser sediment layer within the mud might originate from diagenetic carbonate formation in association with methane oxidation (Paull et al., 1992). This diagenetic mineral formation thus may have created a cap rock that might act as trap for gas. However, upon analysis of several samples within, above, and below the denser layers with a scanning electron microscope equipped with an energy-dispersive X-ray detector, we found no evidence for carbonate formation, or any compositional differences or differences in mineral assemblages.

In conclusion, the results of investigations into sediment physical properties indicate that the wet bulk density of the diatomaceous mud is exceedingly low. Contrary to our expectations, we found no systematic change in sediment density associated with observed or inferred upper limits of free gas.

4. Discussion

Seasonal occurrence of H_2S -rich waters and associated fish kills and lobster walk-outs are part of the folk lore in the area of Swakopmund and Walvis Bay (Copenhagen, 1953). They typically occur during austral summer (November to March) and are characterized by localized discolorations of the sea surface (turquoise to khaki-green), intensive smell of H_2S . Sulfide outbreaks are suspected to be a major influence on coastal and pelagic habitats in the shelf ecosystem, because H_2S is a potent respiratory toxin (Bailey et al., 1985; Classen, 1930; Copenhagen, 1953).

Geographical regions on the shelf with the highest incidence of observed eruptions coincide with nursery grounds of important pelagic and demersal fish; in 1992/1993 half of the recruit population of cape hake (two billion individuals) may have been eradicated by anoxic conditions, possibly in connection to sulfide eruptions (Hamakuya et al., 1998; Weeks et al., 2002).

The discussion focuses on two issues. First is the origin of hydrogen sulfide and methane gas in light of our new findings, where we dispute the traditional explanation of anoxia and H₂S eruptions over the shelf offshore Namibia. Second is the question of what external or internal trigger may cause gas eruptions from sediments.

4.1. Origin of gas: water column versus sediment

The eruption intensity and frequency appears to vary between years, and are regionally focused over the wide shelf offshore of Walvis Bay and Swakopmund. According to a recently initiated observation program by NATMIRC, eruptions occur most frequently after inland rains, a feature that will be discussed later. The original and still commonly accepted scientific hypothesis is that these events are due to H₂S generation in water over the shelf. This was (to our knowledge) first formulated by Copenhagen (1953) and later refined by Hart and Currie (1960) and Bailey (1991). This hypothesis attributes anoxia and H₂S liberation to an interplay between regional-scale meteorological processes associated with the trade wind system, changes in the water mass structure over the shelf, and biological processes.

4.2. The oceanographic/biological hypothesis

The high biological productivity in the euphotic zone overlying the shelf off Namibia (Steeman Nielsen and Jensen, 1957) results in high oxygen consumption rates in waters below the thermocline and at the sea floor. Three hydrographic features of this upwelling system are important with respect to the oxygen supply for shelf water: The first is the poleward undercurrent that compensates the northward component of the Ekman transport. It is fed by South Atlantic Central Water (SACW)

originating in the area of the Angola Dome—an oceanic area with old and oxygen-depleted waters (Chapman and Shannon, 1987)—and arrives offshore Namibia with oxygen concentrations well below 90 µM. The second feature is landward advection of Eastern South Atlantic Central Water (ESACW) in a deep compensation current balancing the offshore Ekman transport. This water mass typically has oxygen concentrations of 178 µmol/l and originates in the source region of the Benguela Current near the Cape of Good Hope. It is transported northwards along the upper slope at water depths of <400 m. Advection of this water mass onto the shelf as an onshore compensation current below the thermocline is forced by the offshore component of the Ekman transport. A third water mass which has considerable effects on the phenomena described here is warm tropical surface water normally found north of the Angola–Benguela Front, usually situated near 17°S. Under specific conditions—outlined below—it is advected southward along the coast to the area off Walvis Bay (and sometimes even further south).

Decreases in trade wind intensity disrupt the oxygen balance over the shelf by altering currents. The cross-shelf compensation current of ESACW reacts instantaneously to changing trade-wind intensity and is immediately interrupted when the trade winds stop. In other words, the most important oxygen source for waters overlying the shelf is directly coupled to fluctuations in the coast-parallel component of the wind field. Only the poleward undercurrent, which has a longer response time, remains to counteract oxygen consumption in the water column and the sediment. However, this water mass is already depleted in oxygen. In addition, oxygen consumption may be enhanced, because stabilization of the water column and stratification after weakening of the upwelling promote plankton blooms over the shelf (Bailey, 1991). Oxygen levels over the shelf can only increase after the trade winds resume, turning on the cross-shelf “conveyer” of oxygen and at the same time force H₂S-laden waters to upwell.

Characteristic features of eruptions caused by this process thus should be linked to lessening

trade wind intensity, with a characteristic time lag of approximately one week between relaxation of wind intensity and the development of anoxia in shelf bottom waters. After renewed trade wind activity, H₂S-laden surface waters should be relatively cold (SACW type), and should occur over spatial scales on the order of tens of kilometers.

Several eruption features cannot be explained by this mechanism. One key phenomenon in the context of H₂S eruptions that previously has not been adequately credited is the occasional emergence of ephemeral mud islands and sea mounds offshore Pelican Point in the years 1884 (report of anomalous sea floor sounding published in the *South African Pilot*, No. 2 of 1884, pages 208–210), 1900, 1959 and 2000 (Waldron, 1901). The only documentation and scientific account available to us is by Waldron (1901): In June of 1900 an island (50 m long, 10 m wide and 5 m high) composed of unconsolidated diatomaceous ooze was observed in waters 15 m deep offshore Pelican Point (22°53'S/014°26'E). “A very strong odour of sulfuretted hydrogen pervaded the spot and steam appeared to issue from the northern end of the mass”, “...the smell from the island was noticed at Swakopmund, a distance of 25 miles from Walvis Bay” and “...dirty appearance of the water with bubbles on the surface...” (Waldron, 1901). A brave-hearted lieutenant, who swam to the island, reported that the water around it was very cold. The island had disappeared entirely by June 7 of 1900. The phenomenon requires mud outflow or eruption at the sea floor, driven by processes beneath the sediment–water interface. The phenomenon differs from mud diapirs known from other submarine settings (Hovland and Curzi, 1989; Hovland and Judd, 1988) in that the uplifted material was the very young diatomaceous mud of Holocene age that is not tectonically or gravitationally overpressured.

An additional fact that is difficult to reconcile with the oceanographic hypothesis is the initially small dimension (less than 1 km diameter) of discrete surface sea water discolorations by elemental sulfur particles (Weeks et al., 2002). This observation argues for an initially localized source of either elemental sulfur or H₂S, which is then oxidized.

4.3. The methane eruption hypothesis

Our alternative and preferred hypothesis proposes that gas accumulates in the pore space of diatomaceous mud and erupts under specific conditions to deliver a mixture of methane and H₂S to the water and to the atmosphere. The geological and geochemical results presented suggest that gas-charged sediments occur most frequently in areas with the highest sediment accumulation rates with the thick layer of diatomaceous mud offshore Walvis Bay and Swakopmund having the largest accumulations. At high sedimentation rates, the sulfate gradients into the sediments are steep so that the zone of methane production is situated close to the sediment–water interface (Berner, 1980). The acoustic and pore water studies indicate that free gas is present in the pore space of the unconsolidated diatomaceous mud, which has low bulk density and low shear strength. These initial gas accumulations are composed predominantly of methane produced during late stages of anaerobic microbial degradation of organic matter (Claypool and Kvenvolden, 1983). H₂S, the product of bacterial reduction of sulfate, is also present in the gas phase. The formation of gas-filled voids decreases the density of lower sediment layers and creates buoyancy. If the gas-filled sediment behaved like a liquid, a density inversion caused by the buoyancy of free gas would cause the sediment to be mobilized. While the shear strength of the diatomaceous mud counteracts mobilization, increased pore fluid pressure decreases the shear strength. However, the observed eruptions have a seasonal pattern and, to our knowledge, do not occur in the random manner expected from gas-driven sediment overturning.

4.4. Possible causes for eruptions

What causes the eruptions to occur at a specific time of year with considerable inter-annual differences in eruption intensity? It is clear that the trigger for eruptions should affect the balance of overburden pressure, sediment shear strength, and internal gas pressure or gravitational instability. The gas is confined either by denser layers in the

sediments (cap “rocks”), or merely by the coupled effects of overburden pressure and shear strength. However, there are numerous possible external influences on the pressure balance, and internal microbiological processes may also play a role. In the following, we review the most likely candidates: (1) the trade-wind system and its effects on the coupled hydrographic and biological conditions in the water column and (2) influences of weather patterns that are connected to low trade-wind phases. Finally, we speculate on the possible role of microbial processes in the sediment. Our evidence at this point is far from conclusive and these influences are at the moment based on conjecture.

4.5. Climatic/oceanographic control

Wind stress is seasonal in the northern Benguela region and imposes considerable seasonality on upwelling and biological production. In addition to seasonal variations, interannual variations are imparted to the coastal upwelling system by changes in trade-wind intensity (Shannon and Nelson, 1996). They arise from variations of the St Helena anti-cyclone and cause variations in trade wind intensity, which in turn acts on the equatorial current system and the Benguela Current (Hagen et al., 2001). The westward equatorial trade winds tend to drive warm surface waters towards the western tropical Atlantic. The westward transport is balanced by eastward counter-currents that feed water into the Gulf of Guinea. The majority of this water is deflected southward by the African coast and is entrained into the permanent poleward undercurrent that compensates the eastern boundary current. The tropical and eastern boundary current water masses meet at the Angola–Benguela Front that is usually located between 14°S and 17°S (Meeuwis and Lutjeharms, 1990; Shannon and Nelson, 1996).

During years with weak SE trade wind intensity the Intertropical Convergence Zone is displaced southwards, and an equatorial Kelvin wave transports warm, saline waters from the western tropical Atlantic to the Gulf of Guinea. This analogue to the El Niño in the Pacific (Shannon

et al., 1986) are called Benguela Niño and have approximately the same temporal recurrence as their Pacific counterpart. This warm surface water is deflected southwards by the African Coast, penetrates the Angola–Benguela Front with warm surface water masses along the coast and reaches as far South as 25°S, causing positive sea-level changes of up to 5 cm at Walvis Bay (Shannon and Nelson, 1996).

In the northern sector of the coastal upwelling system (17°30' S to 25°S, approximately 15–30 km wide and characterized by SST of 14°C) the inflow of warm waters raises SST by 2°C to 8°C (Shannon and Nelson, 1996). The increased SST causes increased evaporation and atmospheric convection: small atmospheric cyclones mark the track of the warm water and lead to increased precipitation on land. The biological consequence of inhibited upwelling is a drastic decrease in phytoplankton productivity, lasting no more than 10 days. The immediate effects of the Benguela Niños on the pressure at the sediment–water interface thus are the sum of (decreased) atmospheric pressure and a 5-cm increase in sea level. The resulting combined effect is negligible considering that eruptions may occur in 100 m water depth. In addition, this effect is counteracted by a decreased flux of organic matter to the sediment, which would tend to reduce oxygen consumption at the sediment surface.

Ongoing in situ measurements with a mooring on the shelf 5 km offshore from Swakopmund (position 22°41.05'S and 14°28.46'E in 30 m water depth) also discount increases in water temperature as a likely cause for eruptions. Such increases would possibly propagate into the sediment and expand the gas volume. Situated in the immediate vicinity of an eruption that occurred offshore Swakopmund on February 15, 2001, the sensor at 25-m water depth did not register a change in water temperature—it remained at 13.2–13.4°C in the entire period from February 9–16, 2001. (The recorded data is held in the environmental database of the Ministry of Fisheries and Marine Resources, Namibia.) In contrast, historical reports suggest that the waters around the mud islands were generally colder than normal during events (Copenhagen, 1953).

Waves and swells have significantly more potential to change the pressure on the sediment: Swell height from southwesterly to westerly directions typically is between 1 and 3 m and wave length is of the order of 150 m (Wannasurf, 2001); it thus has the potential to reach sea floor shallower than 75 m water depth. However, in some locations around Swakopmund such conditions are found for >150 days per year and thus would not explain the observed seasonality in eruptions.

Since oceanographic explanations are lacking, we turn to two processes that may indirectly change the pressure balance in the sediment.

4.6. Biological control

Aside from physical processes, two specific biological processes are very important to the control the hydrogen sulfide concentrations in sediment pore waters and the water column: (1) The production of hydrogen sulfide in the sediments by sulfate-reducing bacteria; (2) The consumption of hydrogen sulfide at the sediment/water interface and in the water column by sulfide-oxidizing organisms. A recent study of sulfate reduction and sulfide oxidation on the Namibian shelf and slope established that hydrogen sulfide production in the top 10 cm of sediment is sufficient to account for the hydrogen sulfide flux across the sediment–water interface (Brüchert et al., 2003). The gradient of hydrogen sulfide is maintained by high sulfate reduction rates, which are sustained by the high accumulation rates of organic matter on the shelf. Because the diatomaceous mud contains little reactive iron to precipitate hydrogen sulfide, the sediment is quickly saturated with respect to hydrogen sulfide and concentrations of sulfide steadily increase with depth until all sulfate is consumed. Although a slow bacterial process, anaerobic oxidation of methane with sulfate converts all remaining sulfate to hydrogen sulfide and thus is the largest contributor to the pore water pool of hydrogen sulfide. Under normal circumstances, the anaerobic oxidation of methane by sulfate in the Namibian shelf sediments removes more than 99% of the methane diffusing upwards. In areas with free gas, the

sulfate-methane transition usually occurs 1 m below the sediment surface. This “biological filter” may fail if the rate of upward methane transport or the production rate exceed the rate of methane oxidation.

Consumption of hydrogen sulfide in the Namibian shelf sediments is mediated by the large sulfur- and nitrate-storing sulfur bacteria *Thiomargarita namibiensis*, *Thioploca* spp., and *Beggiatoa* spp. (Schulz et al., 1999). The distribution of *Thiomargarita* is linked to the presence of free gas in the sediment (Vogt, 2002). Since *Thiomargarita* is not motile, a regular recharge of its intracellular nitrate stock requires that the bacterium is passively moved to environments where nitrate is abundant. Sedimentary gas eruptions would provide a transport mechanism, and may explain the spatial coincidence of observed eruptions and bacterial populations (Vogt, 2002). *Thiomargarita* has been estimated to account for as much as 55% of the total sulfide oxidation (Brüchert et al., 2003), which emphasizes their important ecological role. Only *Thiomargarita* appears to tolerate environments with high concentrations of hydrogen sulfide. The possible feed-back mechanisms from this sulfide-oxidizing consortium to the methane-oxidizing consortia that may influence rates of methane oxidation and pore water gradients are unknown. Whereas it is entirely possible that the bacterial assemblage benefits only passively from the eruptions without having an active role in triggering them, any change in the rates of methane production and oxidation by microbial consortia would affect the methane gradient and potentially cause eruptions.

4.7. Climatic control, II

A final hypothesis links gas eruptions to inland rains, which according to observations invariably accompany phases of H₂S outbreaks. The near-coastal low-pressure troughs linked to the ingressions of warm, tropical water masses bring localized rains to parts of the Namibian coast and inland mountains. Precipitation (up to 60 mm/day) is collected and channelled into wadis that either discharge into the ocean, or disappear under the famous sand dunes of the Great Namib Desert

(Christelis and Struckmeier, 2001). One of these is the Kuiseb River that disappears in the highly porous dune sands inland close to Walvis Bay before reaching the sea. River beds were incised on the shelf during the last glaciation; today, these drowned valleys are filled with alluvial sediments and are extensively mined for diamonds in southern Namibia. We hypothesize that such river beds filled with highly porous sands and gravel deposits also underlie the Holocene diatomaceous muds in the area offshore Swakopmund and Walvis Bay. Near coastal and submarine freshwater discharges are a common feature of the coast near Walvis Bay (Reuning, 1925). We postulate that aquifers at the base of the diatomaceous mud may transmit a hydraulic pressure signal of rising water tables in the aquifers to the base of the mud, triggering eruptions of barely contained sedimentary gas accumulations.

5. Conclusions

Outbreaks of toxic H₂S gas are a seasonally (austral summer) recurrent feature in the near-coastal shelf environment offshore Namibia. They have a significant economic and societal relevance because of their effects on biota in one of the largest marine coastal upwelling regions (fisheries being the third largest source of revenue for Namibia). Until recently they were considered to be of local geographical extent and forced by a combination of high biological productivity in combination with reduced advection of oxygenated ocean water. Ship-borne acoustic surveys in 2000 suggest a significant contribution by eruptions of biogenic gas (methane and H₂S) from the sea floor: An area of approximately 1500 km² of unconsolidated organic-rich diatomaceous ooze on the shelf is gas-charged to within 100 cm below the sediment–water interface. The sedimentary gas accumulations contain a highly toxic mixture of methane and H₂S and eruptions of that gas may be a reason for large-scale fish kills known from the area. As yet the triggering mechanisms have not been identified, but processes that may be responsible include mud diapirism forced by buoyancy, increases in pore pressure by submarine freshwater

discharge, changes in the rate of microbial methane oxidation, or changes in the water column pressure at the sea floor.

Acknowledgements

We thank captain and crew of F/S *METEOR* for an enjoyable time offshore Namibia and the Namibian authorities and NATMIRC for excellent co-operation. Helpful reviews by L.I. Dimitrov, A.D. Judd, K.A. Kvenvolden, and I. Leifer are gratefully acknowledged. Funding was obtained from the German Research Foundation under Grants EM37-10/1, EM37-16/1, and EM37-17/1 to the senior author.

References

- Bailey, G.W., 1991. Organic carbon flux and development of oxygen deficiency on the modern Benguela continental shelf south of 22°S: spatial and temporal variability. In: Tyson, R.V., Pearson, T.H. (Eds.), *Modern and Ancient Continental Shelf Anoxia*. The Geological Society, London, pp. 171–183.
- Bailey, G.W., De Beyers, C.J., Lipschitz, S.R., 1985. Seasonal variation of oxygen deficiency in waters off southern South West Africa in 1975 and 1976 and its relation to the catchability and distribution of the Cape rock lobster Jasus lalandii. *South African Journal of Marine Science* 3, 197–214.
- Berner, R.A., 1980. *Early Diagenesis: A Theoretical Approach*. Princeton University Press, Princeton, NJ, 241pp.
- Bremner, J.M., 1983. Biogenic sediments on the SW African (Namibian) continental margin. In: Thiede, J., Suess, E. (Eds.), *Coastal Upwelling: Its Sediment Record. Part B: Sedimentary Records of Ancient Coastal Upwelling*. Plenum Press, New York, pp. 610.
- Brüchert, V., Jørgensen, B.B., Neumann, K., Riechmann, D., Schlosser, M., Schulz, H., 2003. Regulation of bacterial sulfate reduction and hydrogen sulfide fluxes in the central Namibian coastal upwelling zone. *Geochim. Cosmochim. Acta* 67, 4505–4518.
- Chapman, P., Shannon, L., 1987. Seasonality in the oxygen minimum layers at the extremities of the Benguela system. *South African Journal of Marine Science* 5, 11–34.
- Christelis, G., Struckmeier, W., 2001. Groundwater in Namibia—An Explanation to the Hydrogeological Map. John Meinert Printing, Windhoek, 128pp.
- Classen, T., 1930. Periodisches Fischsterben in Walvis Bay, South West Africa. *Palaebiologica* 111, 13.

- Claypool, G.E., Kvenvolden, K.A., 1983. Methane and other hydrocarbon gases in marine sediment. Annual Review of Earth and Planetary Sciences 11, 299–327.
- Cline, J.D., 1969. Spectrophotometric determination of hydrogen sulfide in natural waters. Limnology and Oceanography 14, 454–458.
- Copenhagen, W.J., 1953. The periodic mortality of fish in the Walvis region—a phenomenon within the Benguela Current. Investigational Report Division of Fisheries-Union of South Africa 14, 1–35.
- Ferdelman, T.G., Fossing, H., Neumann, K., 1999. Sulfate reduction in surface sediments of the southeast Atlantic continental margin between 15°38'S and 27°57'S (Angola and Namibia). Limnology and Oceanography 44 (3), 650–661.
- Hagen, E., Feistel, R., Agenbag, J.J., Ohde, T., 2001. Seasonal and interannual changes in intense Benguela upwelling (1982–1999). Oceanologica Acta 24 (6), 557–568.
- Hamakuya, H., O'Toole, M., Woodhead, P.M.J., 1998. Observations of severe hypoxia and offshore displacement of Cape Hake over the Namibian shelf in 1994. In: Benguela dynamics: Impacts of Variability on Shelf-sea Environments and Their Living Resources. South Afrircan Journal of marine Science, 19, 41–57.
- Hart, T.J., Currie, R.I., 1960. The Benguela Current. Discovery Reports XXXI, 123–298.
- Hovland, M., Curzi, P., 1989. Gas seepage and assumed mud diapirism in the Italian central Adriatic Sea. Marine and Petroleum Geology 6, 161–169.
- Hovland, M., Judd, A.G., 1988. Seabed Pockmarks and Seepages. Graham and Trotman, London, 293pp.
- Meeuwis, J.M., Lutjeharms, J.R.E., 1990. Surface thermal characteristics of the Angola Benguela Front. South African Journal of Marine Science 9, 261–279.
- Paull, C.K., et al., 1992. Indicators of methane-derived carbonates and chemosynthetic organic carbon deposits: examples from the Florida Escarpment. Palaios 7, 361–375.
- Reuning, E., 1925. Gediegen Schwefel in der Küstenzone Südwesterafrikas. Centralblatt für Mineralogie A (3), 86–94.
- Schulz, H.N., et al., 1999. Dense populations of a giant sulfur bacterium in Nambian shelf sediments. Science 284, 493–495.
- Shannon, L.V., Boyd, A.J., Brundrit, G.B., Taunton-Clark, J., 1986. On the existence of an El Nino type phenomenon in the Benguela system. Journal of Marine Research 44, 495–520.
- Shannon, L.V., Nelson, G., 1996. The Benguela: large-scale features and processes and system variability. In: Wefer, G., Berger, W.H., Siedler, G., Webb, D.J. (Eds.), The South Atlantic: Present and Past Circulation. Springer, Berlin, pp. 163–210.
- Spieß, V., 1993. Digitale Sedimentechographie—Neue Wege zu einer hochauflösenden Akustostratigrafie., Ber. FB Geowissenschaften Bremen, 35, Bremen.
- Steeman Nielsen, E., Jensen, E.A., 1957. Primary oceanic production. The autotrophic production of organic matter in the oceans. Galathea Reports 1, 49–136.
- Vogt, T., 2002. Akustische Fazies auf dem Schelf und oberen Kontinentalrand vor Namibia—Auswertung von PARASOUND-Ergebnissen der Reise METEOR 48-2. M.Sc. Thesis, University of Greifswald, Greifswald, 80pp.
- Waldron, F.W., 1901. On the appearance and disappearance of a mud island at Walvis Bay. Transactions of the South African Philosophical Society XI, 185–188.
- Wannasurf, 2001. http://www.wannasurf.com/spot/Africa/Namibia/cape_cross/index.html.
- Weeks, S., Currie, B., Bakun, A., 2002. Massive emissions of toxic gas in the Atlantic. Nature 415, 493–494.